Progress in Neuropsychopharmacology & Biological Psychiatry 116 (2022) 110533

Contents lists available at ScienceDirect

Progress in Neuropsychopharmacology & Biological Psychiatry

journal homepage: www.elsevier.com/locate/pnp

Multimodal MRI reveals alterations of the anterior insula and posterior cingulate cortex in bipolar II disorders: A surface-based approach

Shufei Zhang [a,1], Ying Wang [b,1,**], Senning Zheng [a], Carol Seger [a,d], Shuming Zhong [c], Huiyuan Huang [a], Huiqing Hu [a], Guanmao Chen [b], Lixiang Chen [a], Yanbin Jia [c], Li Huang [b], Ruiwang Huang [a,*]

[a] School of Psychology, Center for the Study of Applied Psychology, Key Laboratory of Mental Health and Cognitive Science of Guangdong Province, South China Normal University, Guangzhou 510631, China
[b] Medical Imaging Center, First Affiliated Hospital of Jinan University, Guangzhou 510630, China
[c] Department of Psychiatry, First Affiliated Hospital of Jinan University, Guangzhou 510630, China
[d] Department of Psychology and Program in Molecular, Cellular, and Integrative Neuroscience, Colorado State University, Fort Collins, CO 80523, USA

ARTICLE INFO

Keywords:
Depression
Superficial white matter (SWM)
Surface-based analysis (SBA)
Resting-state functional connectivity (RSFC)

ABSTRACT

Background: Bipolar disorder (BD) is a mental disorder with severe implications for those affected and their families. Previous studies detected brain structural and functional alterations in BD patients. However, very few studies conducted a multimodal MRI fusion analysis, and little is known about the role of common anomalies in the connectivity of BD.

Methods: We collected sMRI, rs-fMRI, and DTI data from 56 patients with unmedicated BD-II depression and 72 age-, sex- and handedness-matched healthy controls. We applied data-driven approaches to analyze multimodal MRI data and detected brain areas with significant group differences in cortical thickness (CT), amplitude of low frequency fluctuations (ALFF), and fractional anisotropy (FA) of the superficial white matter. We observed the common abnormal areas and took these areas as seeds to analyze the resting-state functional connectivity (RSFC) patterns in BD patients by overlapping these abnormal areas.

Results: The BD patients showed two common abnormal areas: (1) the left anterior insula (AI) with abnormal CT and FA, and (2) the left posterior cingulate cortex (PCC) with abnormal CT and ALFF. Seed-based analyses showed RSFC between the left AI and left occipital sensory cortex, the left AI and left superior and inferior parietal cortex, and the left PCC and right medial prefrontal cortex were uniformly lower in the BD patients than controls. Correlation analyses showed negative correction between AI's FA and disease episodes and between AI's FA and disease duration in depressed BD-II patients.

Conclusions: We observed abnormal brain structural and functional properties in the left AI and left PCC in BD patients. The abnormal RSFC patterns may suggest sensory and cognitive dysfunction in BD.

1. Introduction

Bipolar disorder (BD) is a severe psychiatric disorder characterized by depressive, manic, or hypomanic episodes (Merikangas et al., 2011; Phillips and Kupfer, 2013). It includes BD type I (BD-I), type II (BD-II), cyclothymic disorder, and BD other not specified (Phillips and Kupfer, 2013) according to the DSM (Association, 2000). Patients with BD, especially BD-II, are frequently misdiagnosed as unipolar depression

Abbreviations: ALFF, amplitude of low frequency fluctuations; CT, cortical thickness; FA, fractional anisotropy; RSFC, resting-state functional connectivity; BD, bipolar disorder; HCs, healthy controls; AI, anterior insula; PCC, posterior cingulate cortex; SPC, superior parietal cortex; IPC, inferior parietal cortex; LOC, lateral occipital cortex; LG, lingual gyrus; FG, fusiform gyrus; mPFC, medial prefrontal cortex; vmPFC, ventromedial prefrontal cortex; MOF, medial orbitofrontal cortex; SFC, superior frontal cortex; rACC, rostral anterior cingulate cortex; SN, salience network; DMN, default mode network; VAN, ventral attention network; DAN, dorsal attention network.

* Corresponding author at: School of Psychology, South China Normal University, Guangzhou 510631, China.
** Corresponding author at: Medical Imaging Center, First Affiliated Hospital of Jinan University, Guangzhou 510630, China.
E-mail addresses: johneil@vip.sina.com (Y. Wang), ruiwang.huang@gmail.com (R. Huang).
[1] These authors contributed equally to this work.

https://doi.org/10.1016/j.pnpbp.2022.110533
Received 1 April 2021; Received in revised form 29 November 2021; Accepted 5 February 2022
Available online 11 February 2022

(Hirschfeld et al., 2003). They spend more time experiencing depressive episodes than manic/hypomanic episodes (Judd et al., 2003; Phillips and Kupfer, 2013). In the past decades, neuroimage techniques have been used to identify objective neurobiological markers corresponding to BD-II. However, the results from previous studies are inconsistent, and the neurophysiological mechanism underlying BD-II remains unclear (Wang et al., 2019a, 2019b).

Magnetic resonance imaging (MRI) has been widely used to explore neurobiological mechanisms and pathophysiology of BD-II. Brain structural MRI (sMRI) has been widely used to detect the structural morphology of brain tissues. Based on the sMRI data, previous studies analyzed gray matter (GM) morphometric properties such as cortical thickness (CT) in patients with BD-II (Abé et al., 2016; Ha et al., 2009; Hibar et al., 2018; Maller et al., 2014). With the voxel-based morphometry (VBM) method, for example, Ha et al. (2009) found lower GM volume in the bilateral ventromedial prefrontal cortex (vmPFC) and the right superior frontal cortex (SFC) in patients with BD-II than controls. By estimating cortical thickness, Abé et al. (2016) found thickness in the bilateral frontal, temporal and medial occipital cortices in patients with BD-II than controls. Moreover, Abé et al. (2018) also reported a focal association between the thickness of the medial prefrontal cortex (mPFC) and the executive function in patients with BD-II.

Functional MRI is also widely used to analyze brain activity and inter-regional functional connectivity (FC) alterations in BD-II patients (Caseras et al., 2013; Gong et al., 2019; Vizueta et al., 2012; Wang et al., 2019a, 2019b; Wang et al., 2016). For example, using the task-related fMRI technique, previous studies found that patients with BD-II showed significantly lower activation in the bilateral vlPFC and right amygdala in response to emotion-processing tasks (Vizueta et al., 2012) and higher activation in ventral striatal areas when subject attending reward-paradigm tasks (Caseras et al., 2013) compared to healthy controls. Previous studies using resting-state fMRI (rs-fMRI) detected abnormal intrinsic activity and resting-state functional connectivity (RSFC) in patients with BD-II. For example, by calculating the square root of the power spectrum of the frequency range (Yang et al., 2007), Zhong et al. (2019) used amplitude of low frequency fluctuations (ALFF) to assess spontaneous brain activity and found lower ALFF in the precuneus/posterior cingulate cortex (PCC) in patients with BD-II than in healthy controls. By calculating whole-brain RSFC, Wang et al. (2016) found that patients with BD-II showed the disrupted RSFC in the default mode network (DMN) and limbic system. Wang et al. (2019a, 2019b) estimated dynamic RSFC based on the triple-network model (Menon, 2011) and found abnormal dynamic functional connectivity between the DMN and ECN.

Diffusion tensor imaging (DTI) allows mapping the diffusion process of water molecules in brain tissues in vivo and non-invasively. According to water molecule diffusion patterns or diffusion properties, we can reveal microscopic details about tissue architecture, either normal or in a diseased state. Several studies (Ambrosi et al., 2016; Ambrosi et al., 2013; Kurumaji et al., 2017; Maller et al., 2014) analyzed the integrity of brain white matter (WM) in patients with BD-II using tract-based spatial statistics (TBSS) and found lower fractional anisotropy (FA) in deeper white matter (WM) bundles such as corpus callosum, inferior longitudinal fasciculus, superior longitudinal fasciculus, internal capsules, cingulate bundles, and anterior thalamic radiations in patients with BD-II than controls. These studies almost focused on the deep WM (DWM) and rarely considered the superficial WM (SWM) (Guevara et al., 2017; Oishi et al., 2008).

In contrast to the DWM, the SWM consists of U-shape fibers, lies beneath the cortex, and mediates the local/short-range connections between intracortical gyri (Guevara et al., 2020; Ji et al., 2019). Moreover, the SWM is the last place to be myelinated that may have high plasticity and vulnerability to diseases (Phillips et al., 2016b). Several recent studies on BD-II (Hong et al., 2018; Liu et al., 2016; Nazeri et al., 2013; Nazeri et al., 2015; Phillips et al., 2016a; Zhang et al., 2018) estimated the properties of SWM and indicated its important role in patients with cognitive decline, Alzheimer's disease, epilepsy, bipolar disorder, Schizophrenia, and Autism. Additionally, Liu et al. (2016) and Hong et al. (2018) found that SWM may be a good candidate to link brain structure and function as well as clinical variables in the surface-based analysis (SBA). Meanwhile, the spatial distribution and arrangement features of the SWM make it more suitable to integrate cortical structural and functional changes (Hong et al., 2018; Liu et al., 2016). In the current study, we were motivated to perform a surface-based multimodal MRI fusion analysis to reveal abnormal brain cortical gray matter, spontaneous activity, and cortico-cortical connection in patients with BD-II.

Compared to a unimodal neuroimaging analysis, the multimodal imaging fusion can provide a large amount of information for increasing the clinical applicability of tissue properties in brain structure and function (Calhoun and Sui, 2016). By taking advantage of cross-information (Sui et al., 2014), a fusion analysis across sMRI, rs-fMRI, and DTI may be more informative than a unimodal neuroimaging analysis (Meng et al., 2017; Sui et al., 2018) for identifying biomarkers in clinical populations. Currently, multimodal analyses have been well recognized for biomarker identification in mental disorders (Calhoun and Sui, 2016). For example, Liu et al. (2016) integrated multimodal imaging measures on the SWM surface and showed temporo-limbic SWM anomalies in patients with temporal lobe epilepsy. Hong et al. (2018) extracted multidimensional structural features on the cortical surface and classified different subtypes of autism according to anatomical anomalies patterns. Several studies (Liu et al., 2018; Meng et al., 2017; Sui et al., 2014; Sui et al., 2015; Sui et al., 2018) also applied multimodal neuroimaging data to link brain structural and functional patterns to specify cognitive impairments in patients with schizophrenia by using multivariate fusion methods. These studies collectively suggested that a fusion analysis across multimodal MRI data can be used to identify neuroimaging biomarkers for predicting cognitive deficits in different brain disorders. Although studies on BD-II using a multimodal fusion analysis are few, we may still postulate that if one area displays multimodal brain differences, this area may be more sensitive to BD-II.

Additionally, compared with the volumetric multimodal MRI fusion approach, the surface-based analysis (SBA) (Glasser et al., 2016a; Glasser et al., 2013; Marcus et al., 2013; Oosterhof et al., 2011; Van Essen et al., 2013) has advantages in integrating multimodal measures. Because of high variability in cortical folding across individuals, the volumetric approach may have imprecise spatial localizations in cortical areas (Glasser et al., 2016b). The SBA is generally believed to make more precise spatial localization in cortical areas (Brodoehl et al., 2020; Coalson et al., 2018; Glasser, Smith, et al., 2016), resulting in a better alignment in cortical areas (Glasser et al., 2016b; Robinson et al., 2018; Van Essen, 2004) or a better identification in cortical morphological features (Dale et al., 1999), which lead to better visualization of cortical spatial relationships (Xu et al., 2016).

The current study aimed to use multimodal neuroimages to reveal the brain areas with abnormal structures and functions in depressed BD-II patients. By taking these brain areas as seeds, we attempted to detect its abnormal functional connectivity in the whole brain. Although most unimodal imaging analyses revealed the altered structural (Hanford et al., 2016; Hibar et al., 2018) and functional (Gong et al., 2019; Gong et al., 2020; Wang et al., 2019a, 2019b; Wang et al., 2016) properties of BD-II, the heterogeneous spatial distribution of these results may not provide the precise localization of brain areas with multimodal alterations (Liu et al., 2016). Thus, we performed an exploratory analysis, rather than taking the regions of interest (ROIs) from previous literature, to detect brain areas with multimodal differences between the patients and controls. In specific, the calculations included two steps: (1) detecting the areas with multimodal differences specific to the datasets of BD-II patients using a data-driven approach, and (2) taking the detected areas as the seeds to estimate the changes of functional connectivity in the BD-II patients.

For this purpose, we collected sMRI, rs-fMRI, and DTI data from 56

unmedicated depressed BD-II patients and 72 healthy controls. After the measures of CT, ALFF, and FA were obtained, we integrated them on the cortical surface by using an SBA approach (Glasser et al., 2013). By co-registering these multimodal MRI measures onto the cortical surface in the standard space, we observed the common brain areas with abnormalities in CT, FA, and ALFF in BD-II patients. Moreover, we took these common areas as seeds to detect alterations of brain FC in the BD patients.

2. Methods

2.1. Subjects

A total of 128 subjects, including 56 BD-II patients and 72 healthy controls (HCs), were recruited from the First Affiliated Hospital of Jinan University, Guangzhou. The BD-II patients (33 M/23 F, aged 17–51 years old) were recruited from the Psychiatry Department and were all right-handed. All patients met the BD-II criteria according to the Diagnostic and Statistical Manual of Mental Disorders Fourth Edition (DSM-IV) and were diagnosed by two clinical psychiatrists (YJ with 20-year and SZ with 5-year experience in clinical psychiatry). The exclusion criteria for the BD-II patients were as follows: (a) the presence of any other psychiatric disorders except BD, (b) a history of electroconvulsive therapy, (c) a history of head injury, trauma, neurological disorder, or mental retardation, (d) alcohol or other substance abuse or addiction, and (e) concurrent psychiatric illnesses. Before the MRI scan, all patients were during the medication-free period or didn't receive medication for a minimum of 6 months. The medication primarily includes mood stabilizers (lithium, sodium valproate) and/or anti-depressants (duloxetine or paroxetine). Finally, the BD-II group included both the patients who had never taken medications and the other patients who had stopped taking medications because the medication was less effective or had side effects or personal choices.

The clinical status of each patient was assessed according to the Young Mania Rating Scale (YMRS) (Young et al., 1978) and the Hamilton Depression Rating Scale (HDRS) (Williams, 1988) (with 24 items) during 7 days before the MRI scanning. All the patients were diagnosed as being in the depression phase with YMRS's score $\leq$ 12 and HDRS's score $\geq$ 21.

In addition, we also recruited 72 right-handed, healthy, non-smoking subjects (42 M/30 F, aged 18–58 years old) as the healthy controls. Each healthy subject has been screened or interviewed to exclude a presence of current or history of any psychiatric illness. The subjects were also excluded from the healthy controls if their first-degree relatives had a presence of current or history of any psychiatric illness.

This study was approved by the Institute Research Board of First Affiliated Hospital of Jinan University (FAHJU), Guangzhou. The written informed consent of each subject was acquired before the study.

2.2. Multimodal MRI data acquisition

All MRI data were acquired on a 3 T GE MR750 scanner with an 8-channel phased-array head coil in the Medical Imaging Department of FAHJU.

The sMRI images (1 mm^3 isotropic) were obtained using a T1-weighted inversion recovery (IR)-prepared ("BRAVO") 3D FSPGR (Fast Spoiled Gradient Echo) sequence with parameters tuned to optimize brain tissue contrast. The parameters were as follows: TR = 8.212 ms, TE = 3.22 ms, inversion time = 450 ms, flip angle = 12°, data matrix = 256 × 256, FOV = 256 mm × 256 mm, slice thickness = 1 mm.

The rs-fMRI data were obtained using a single-shot multislice gradient-echo EPI sequence with the following parameters: TR = 2000 ms, TE = 25 ms, flip angle = 90^o, FOV = 240 mm × 240 mm, data matrix = 64 × 64, slice thickness = 3 mm, interslice gap = 1 mm, 35 axial interleaved slices covering the whole brain, and 210 volumes acquired in about 7 min. During the rs-fMRI scanning, each subject was instructed to relax with their eyes closed without falling asleep and without thinking about anything in particular. No subject reported falling asleep during the scan when the subject was asked immediately after the scanning.

The DTI data were obtained using a single-shot multislice spin-echo diffusion-weighted EPI sequence with the following parameters: repetition time (TR) = 8000 ms, echo time (TE) = 68 ms, field of view (FOV) = 256 mm × 256 mm, data matrix = 128 × 128, slice thickness = 2 mm, without inter-slice gap, flip angle = 90°, 30 diffusion-sensitive directions with b = 1000 mm^2/s, 5 volumes with b_0 = 0 mm^2/s, and 75 axial interleaved slices covering the whole brain. Each subject was scanned twice in the same session to improve the signal-to-noise ratio.

For each subject, the sMRI data, rs-fMRI, and DTI datasets were obtained in the same session.

2.3. Data preprocessing

For each subject, we pre-processed the sMRI data to estimate CT, the rs-fMRI data to compute ALFF, and the DTI data to calculate FA. Among these measures, CT was estimated on the cortical surface, while ALFF and FA were obtained on the volumetric space. The procedures are illustrated in Fig. 1.

The sMRI data were preprocessed using an automatic pipeline in FreeSurfer (Ver 5.3) (http://surfer.nmr.mgh.harvard.edu/). The pipeline involved the following steps: 1) intensity normalization, 2) brain extraction, 3) brain segmentation, 4) WM and pial surface tessellation, and 5) CT calculation.

The rs-fMRI data were preprocessed using DPABI (Ver 3.0) (http://rfmri.org/dpabi). The pipeline included the following steps, 1) the first 10 volumes were excluded for magnetization equilibrium, 2) slice-timing correction to correct acquisition time differences between slices, 3) head-movement correction for correcting misalignment across time-points, 4) detrending voxel time-series with linear, quadratic, and cubic trends, and 5) regression of head-movement (Friston-24) parameters, WM and CSF signals. We also excluded images if the head movement >1.5 mm in any plane or rotation >1.5°in any axis, which is only excluded in the rs-fMRI analysis. We excluded 12 subjects (5 patients and 7 healthy subjects) for further analysis. After band-pass filtering the BOLD time-series (0.01–0.1 Hz), we estimated voxel-based ALFF values in the whole brain.

The DTI data were preprocessed using FDT/FSL (Ver 5.0). The pipeline involved the following steps: 1) brain extraction from b_0 images, 2) correction for eddy-current and the head movement induced distortions, 3) rotation of diffusion-sensitive gradient orientations, 4) average of the two DTI datasets to increase SNR, and 5) FA estimation on each voxel in the whole-brain.

2.4. Surface-based analysis

2.4.1. Individual brain volume to cortical surface mapping

Based on the sMRI data, the individual cortical surface was generated using FreeSurfer, and the cortical thickness was obtained. While for individual ALFF and FA maps, we need to map them onto the cortical surface, which is illustrated in Fig. 1a and described as follows separately.

About individual ALFF maps, we first performed a 6-dof boundary-based registration (BBR) between brain functional images and sMRI. In the registration step, we have visually inspected registrations and slightly manually adjusted them to ensure good registration. Then we projected ALFF at the intracortical surface (or SWM), which was above the WM surface with half of the thickness in each vertex. Similarly, for each FA map, we also performed a 6-dof BBR to make transformations between the b_0 images and sMRI and inspected them visually. After the registration, we projected the individual FA map onto the cortical surface by sampling FA values at the cortical surface 2 mm below the WM/GM boundary (mri_vol2surf). Given that SWM, including the U-shape

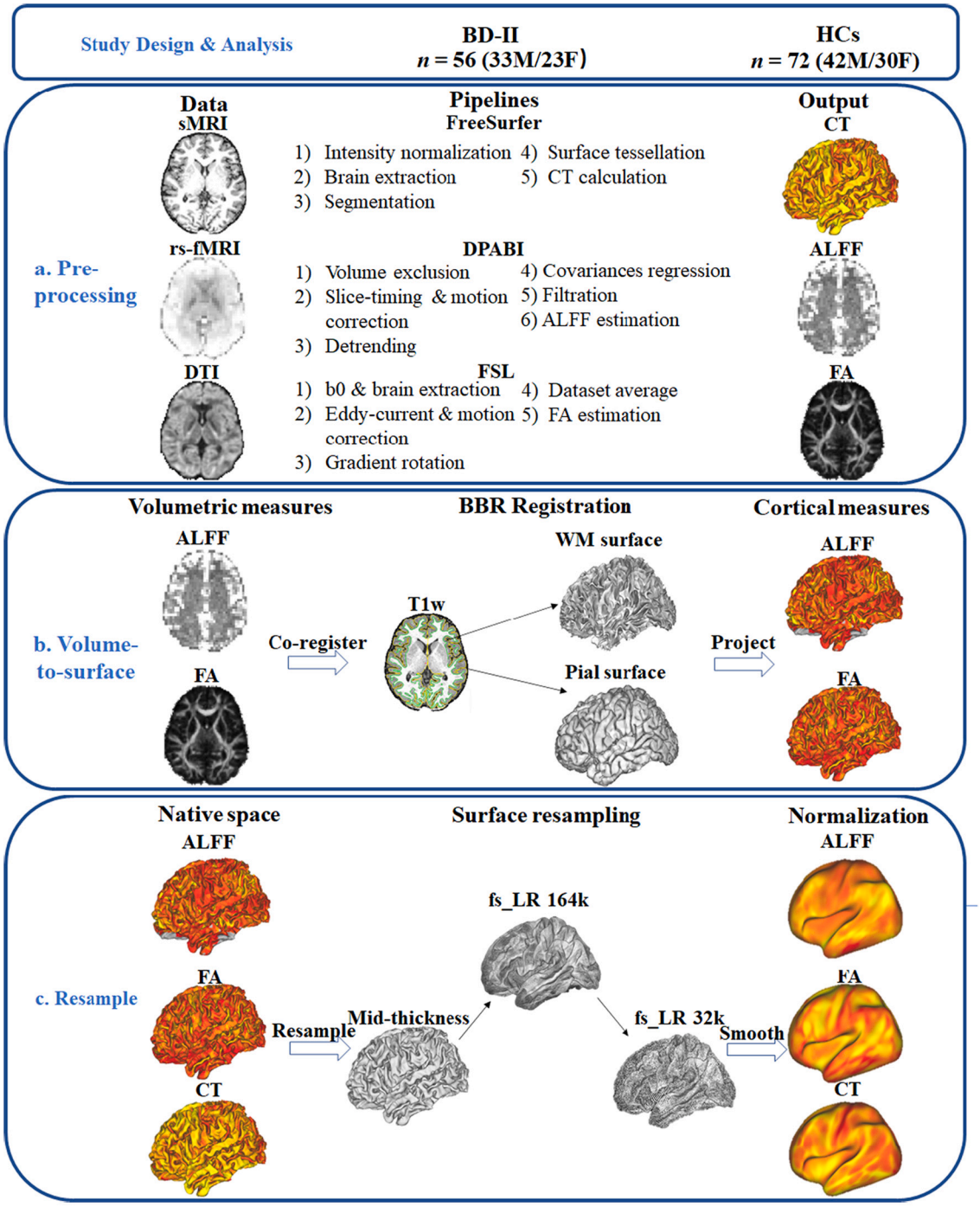

Fig. 1. Pipeline for the surface-based analysis (SBA). (a) rs-fMRI, DTI, and sMRI data were preprocessed through pipelines of DPABI, PANDA, and FreeSurfer. (b) Volume to surface mapping. Using boundary-based registration (BBR), individual ALFF and *b*0 images were co-registered to the brain structural images, and cortical ALFF and FA values were resampled at the intracortical and inner surface (2 mm below the WM surface), separately. (c) Resample. Individual pial and WM surfaces were averaged to create the mid-thickness surface and down-resampled to the fs_LR 32 k surface via the fs_LR 164 k surface. Following the surface resampling calculation, individual multimodal measures were down-resampled onto the fs_LR 32 k surface via the fs_LR 164 k surface. All the measures at the fs_LR 32 k surface were smoothed. Abbreviations: ALFF, amplitude of low frequency fluctuations; FA, fractional anisotropy; FA, fractional anisotropy; *b*0, non-diffusion-weighted images; WM, white matter; CT, cortical thickness; HCs: healthy controls.

WM fibers and termination of deep WM tracts, are located below the WM/GM boundary at a depth of 1.5–2.5 mm (Liu et al., 2016; Schüz and Braitenberg, 2002). In the current study, we re-sampled FA at a depth of 2 mm below the WM surface and assumed the sampled FA reflected diffusion properties of cortico-cortical connections.

2.4.2. *Re-sampling procedure for individual SBA*

For each CT, FA, and ALFF map, we performed the SBA by re-sampling and aligning each of them separately to a standard surface with a suitable resolution. Fig. 1b shows the four steps for the alignment. (i) Individual WM surface and pial surface were averaged to create a mid-thickness cortical surface (intracortical) for each subject (Van Essen, 2012). (ii) Individual mid-thickness surface was re-sampled to a

cortical surface with 163,842 vertices (fs_LR 164 k, vertex spacing = 0.9 mm) and then down-sampled to a cortical surface with 32,492 vertices (fs_LR 32 k, vertex spacing = 2 mm) using the Connectome Workbench software package (Marcus et al., 2013). (iii) Individual CT, ALFF, and FA maps on the cortical surface were separately aligned to the fs_LR 32 k cortical surface from the fs_LR 164 k cortical surface. (iv) Finally, we spatially smoothed each of the measures (CT, ALFF, and FA) separately and time series at the fs_LR 32 k cortical surface with an isotropic Gaussian kernel of $\sigma = 4.25$ mm or full-width-at-half-maximum (FWHM) = 10 mm ($FWHM = \sigma\sqrt{8ln2}$).

2.4.3. Group differences in CT, ALFF, and FA

Using the SBA approach, we first determined the cortical areas with a between-group difference in CT and then determined the cortical areas with between-group differences in ALFF and FA separately (Fig. 2). By overlapping these cortical areas, which showed between-group differences in CT, ALFF, and FA together on the cortical surface, we can detect the common areas with not only abnormal brain structure but also abnormal function in the BD-II patients.

2.4.4. Seed-based analysis of RSFC

By taking the cortical areas with common abnormalities as seeds, we conducted an SBA in the whole brain to reveal abnormal RSFC in BD-II patients.

2.5. Statistical analysis

2.5.1. Demographic information

A two-sample *t*-test was used to evaluate differences in age and educational level between the BD-II patients and the control group. A χ^2-test was used to estimate the gender distribution across groups. The significance level was set at $p < 0.05$ for these tests using SPSS (version 20.0).

2.5.2. SBA statistics

A permutation *t*-test ($n = 10{,}000$ times) was used to compare the between-group differences in each of the measures (CT, ALFF, and FA) at each vertex by using the Permutation Analysis of Linear Models (PALM) package (Winkler et al., 2014; Winkler et al., 2016). In the calculation, we applied a general linear model (GLM) and regressed out the effects of gender, age, and educational level. For multiple comparisons correction, a false discovery rate (FDR) method was applied, and the significance threshold for each measure was set at $p_{FDR} < 0.05$ (approximate to -lg (p_{FDR}) >1.301). Thus, we identified cortical areas with significant between-group differences in CT, ALFF, and FA separately.

By overlapping these cortical areas together, we obtained the intersection areas on the cortical surface. In this way, we determined the common abnormal areas with more than one of the imaging modalities (CT, ALFF, and FA) for the BD-II patients. On the fs_LR 32 k cortical surface, we labeled these areas according to the Desikan-Killiany atlas (Desikan et al., 2006).

To estimate the relationship between the imaging measures and clinical variables, we also mapped the interaction areas from the cortical surface back to the individual functional space and diffusion space separately. For each area, we estimated the averaged values of CT, ALFF, and FA, separately for each subject. The correlation between each imaging measure and each clinical variable was obtained.

2.5.3. Seed-based analysis of RSFC

The SBA of RSFC was performed to detect abnormal RSFC in BD-II patients on the fs_LR 32 k cortical surface (Fig. 3). For each subject, we took each of the intersection areas as a seed to calculate the RSFC map between the seed and the remaining vertices (fs_LR 32 k cortical surface) by using Workbench (wb_command -cifti-average-roi-

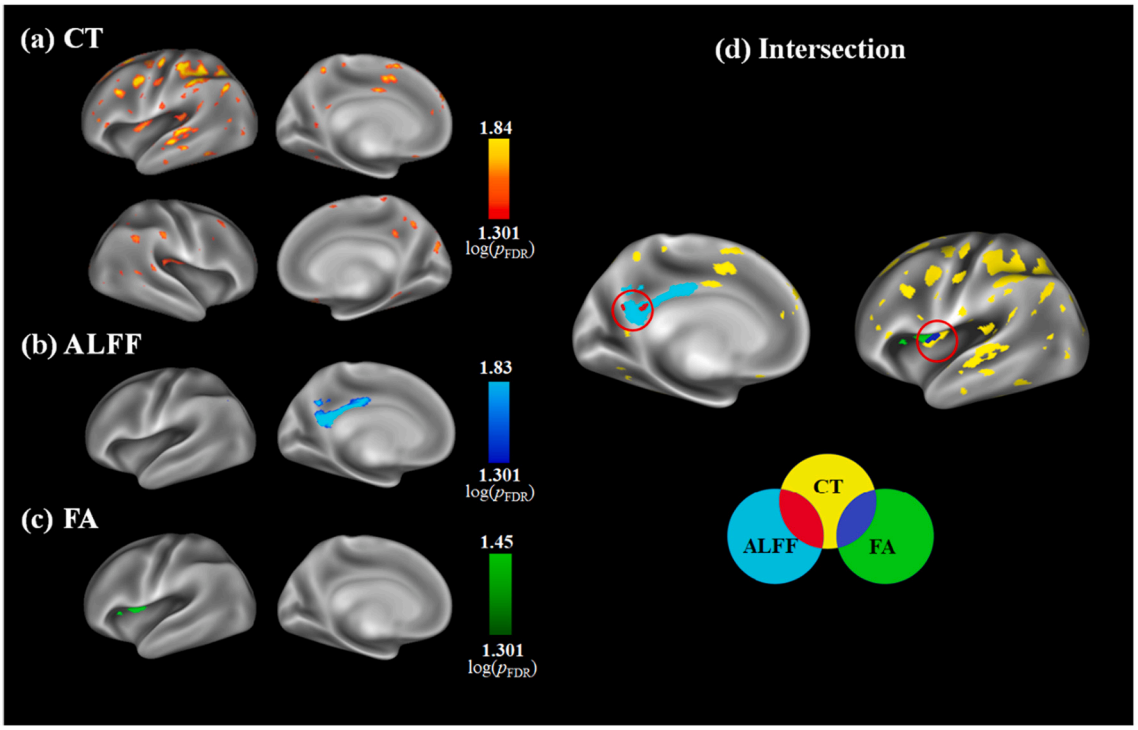

Fig. 2. Surface-based analysis of the abnormal cortical areas in multimodal imaging measures (CT, cortical thickness; FA, fractional anisotropy; ALFF, amplitude of frequency fluctuations) and their overlapping areas. (a) CT, (b) FA, and (c) ALFF. On the fs_LR 32 k surface, the BD-II patients showed lower values in imaging measures (CT, FA, and ALFF) than those in the controls. The results are displayed with a threshold at $p_{FDR} < 0.05$ or ($-\lg(p_{FDR}) > 1.301$). Each color bar represents FDR-corrected *-lg(p)* values for each measure. (d) Intersection areas between CT and FA as well as between CT and ALFF. The BD-II patients showed significantly lower CT and FA in the left AI (blue) and lower CT and ALFF in the left PCC (red) than the healthy controls. (For interpretation of the references to color in this figure legend, the reader is referred to the web version of this article.)

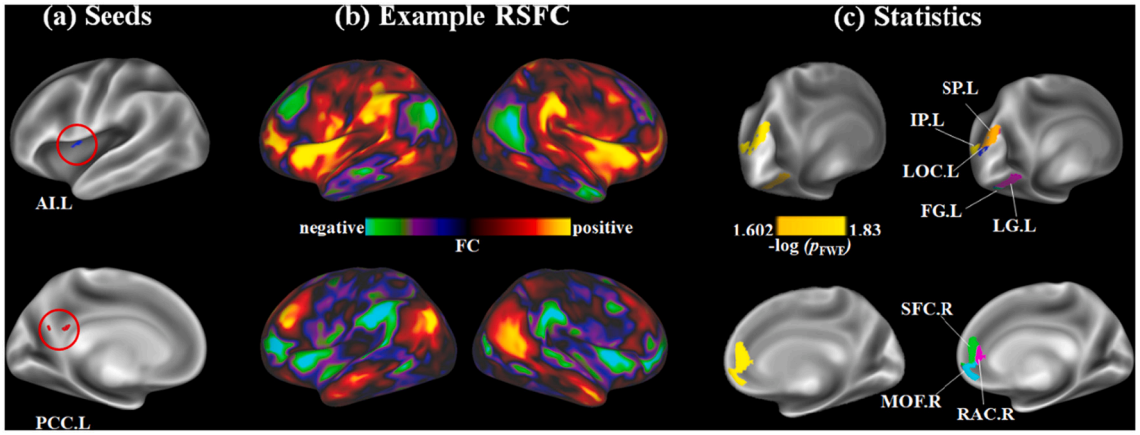

Fig. 3. Seed-based resting-state functional connectivity (RSFC) for patients with bipolar II disorder (BD-II) and healthy controls. (a) Intersection areas were identified in the left anterior insula (AI.L) and left posterior cingulate cortex (PCC.L). (b) Example RSFC maps from the seeds at the AI.L or PCC.L. The color bar indicates the RSFC values in seed-based RSFC maps. (c) Clusters showing significant between-group differences in seed-based RSFC maps ($-lg(p_{FWE/2} > 1.602$), cluster-forming threshold <0.01). BD-II patients showed lower RSFC with two areas for the AI.L seed. The first cluster is located in the left superior parietal cortex (SPC.L), inferior parietal cortex (IPC.L), and the left lateral occipital cortex (LOC.L). The second cluster is located in the lingual gyrus (LG.L) and fusiform gyrus (FG.L). For the PCC.L seed, the BD-II patients also showed lower RSFC for a cluster, which extends across parts of the right rostral anterior cingulate cortex (rACC.R), medial orbitofrontal cortex (MOF.R), and superior frontal gyrus (SFG.R). The color bar represents the $-lg(p_{FWE})$ values. CT: cortical thickness; FA: fractional anisotropy. RSFC: resting-state functional connectivity.

correlation, https://www.humanconnectome.org/software/workbench-command).

A non-parametric permutation *t*-test (10,000 times) was applied to determine between-group differences in RSFC. In the calculations, we took gender, age, and educational level as covariates and regressed them out in GLM. For multiple comparisons correction, cluster-forming threshold and family-wise error (FWE) methods were applied (cluster-forming threshold <0.01, $p_{FWE} < 0.05/n$ with n = times of RSFC statistics) (Winkler et al., 2014; Winkler et al., 2016). In this way, we determined cortical areas showing significant differences in RSFC between the two groups.

2.5.4. Relationship between imaging measures and clinical variables

For each common abnormal cortical area, we assessed the relationship between each imaging measure (CT, ALFF, and FA) and each clinical variable in the patients using partial correlation analyses of SPSS (Ver 20.0). We first extracted the mean value of a relevant measure from a given intersection region and then estimated its correlation with the disease duration (calculating from a first hypomanic or depressive episode), episodes (total past number of hypomanic and depressive episodes), YMRS, and HDRS scores, separately, in the BD-II patients. Considering the confounding effects of demographical variables, we regressed out the gender, age, and educational levels during analyses. The significance level for each correlation test was set at $p_{(two\text{-}tailed)} < 0.05$.

3. Results

3.1. Demographics

Table 1 lists demographic information for each group and clinical information for the BD-II patients. No significant difference was found in either gender or age between the two groups. The BD-II patients had significantly lower educational levels than that of the controls ($p < 0.001$).

3.2. Gender and group interactions

In the study, we set up a general linear model (GLM) to analyze the effect of the interaction between group (BD/HCs) and sex (Male/Female) on the imaging measures with FSL/Feat (https://fsl.fmrib.ox.ac.uk/fsl/fslwiki/GLM). We performed surface-based analyses in CT, ALFF, and FA, separately by using Palm packages (https://fsl.fmrib.ox.ac.uk/fsl/fslwiki/PALM). Unfortunately, we found no statistically significant interaction between group and gender on each of the imaging measures.

Table 1
Demographic information and clinical measures for the bipolar disorder (BD) II depression group.

Parameter	BD-II (n = 56)	Healthy controls (n = 72)	p-value (two-tailed)
Gender	33 M/23 F	42 M/30 F	0.95[a]
Age (years old)	26.0 ± 8.7	27.6 ± 8.5	0.30[b]
Educational level (years)	13.3 ± 3.1	16.0 ± 3.0	< 0.001**[c]
Episodes (number)	2.8 ± 1.7	N/A	
Onset age (years old)	22.1 ± 9.7	N/A	
Duration time (months)	42.8 ± 56.4	N/A	
HDRS	28.8 ± 5.5	N/A	
YMRS	3.3 ± 3.0	N/A	

Abbreviations: HDRS, Hamilton Depression Rating Scale; YMRS, Young Mania Rating Scale; BD, bipolar disorder; HCs, healthy controls; N/A, no record.
Episodes: total past number of hypomanic and depressive episodes; Duration time: calculating from a first hypomanic or depressive episode.
[a]means χ2-test. [b] and [c] mean two-sample *t*-tests. ** means *p*-value <0.01.

3.3. Common cortical areas with abnormal multimodal measures (CT, FA, and ALFF)

Fig. 2 shows the cortical areas with abnormal CT, FA, and ALFF in the BD-II patients and their intersection areas on the cortical surface. We detected two intersection cortical areas in the patients, one in the left PCC and the other in the left anterior insula (AI). That is, the patients showed uniformly lower CT and ALFF in the area at the left PCC and uniformly lower CT and FA in the areas at the left AI than the controls. No cortical area was observed with simultaneously abnormal CT, FA, and ALFF in the BD-II patients.

3.4. Seed-based RSFC

Fig. 3 shows seed-based analysis of RSFC when taking the two common abnormal cortical areas, the left AI and the left PCC (Fig. 2), as the seeds. For the seed at the left AI, the BD-II patients showed significantly lower RSFC than the controls with the connecting clusters in the left parietal and occipital cortices ($p_{FWE} < 0.05$, approximate to -lg($p_{FWE/2}$) >1.602), including the superior parietal cortex (SPC), inferior parietal cortex (IPC), lateral occipital cortex (LOC), lingual gyrus (LG), and fusiform gyrus (FG). While for the seed at the left PCC, the patients showed significantly lower RSFC than the controls with the connecting clusters in the portions of the right mPFC ($p_{FWE} < 0.05$, approximate to -lg($p_{FWE/2}$) >1.602), including the medial orbitofrontal cortex (MOF), rostral anterior cingulate cortex (rACC), and superior frontal cortex (SFC).

3.5. Relationship between imaging measures and clinical variables

In the abnormal cortical areas in the left AI, we found significant negative correlations between FA and the disease duration and between FA and the disease episodes in the BD-II patients according to the partial correction test ($p_{(two\text{-}tailed)} < 0.05$), which is shown in Fig. 4. For the measures of CT and ALFF, no significant correlations were found between any of them and clinical variables in the BD-II patients. However, in the abnormal cortical areas in the left PCC, we found no significant correlations between any of these measures (CT, FA, and ALFF) and clinical variables in the BD-II patients.

4. Discussion

We analyzed brain CT, ALFF, and FA on the cortical surface based on the multimodal MRI data and identified the common abnormal cortical areas associated with BD-II. With the SBA approach, we found two common lateralized abnormal cortical areas, the left AI and left PCC, in the BD-II patients. In addition, by taking the common abnormal areas as the seeds, we found the BD-II patients showed significantly lower RSFC between the left AI and the left superior and inferior parietal and left occipital cortices, and lower RSFC between the left PCC and the right mPFC, than those in the controls.

4.1. Abnormal cortical area in the left AI in depressed BD-II patients

The BD-II patients showed both lower CT and lower FA in the left AI as well as lower RSFC between the left AI and the superior and inferior parietal and occipital sensory cortices than the controls (Fig. 3). The AI is associated with a variety of emotional and cognitive functions. First, the AI is believed to be a crucial region in interoceptive awareness (Craig, 2009), a sense of the bodily physical states, and thought to integrate information of interoception and subjective feelings (Harrison et al., 2010). Studies in healthy populations indicated that the AI is a key region relating to emotion processing and decision making (Craig, 2003; Iaria et al., 2008). The impairment of the AI may be associated with risks in manic decision making in BD (Bora et al., 2010; Ganzola and Duchesne, 2017; Goodkind et al., 2015) and disrupted internal awareness (Craig, 2003). In addition to its roles in emotion processing, as a component of the salience network (SN) and ventral attention network (VAN), the AI is also believed to be involved in the detection and attentional orientation to salient stimuli (Adolfi et al., 2017; Chica et al., 2013). As a major brain hub with extensive connections to other functional networks, including the default mode network (DMN), CEN, affective network, and cortico-striatal network, the AI plays a key role in cognitive and affective integration (Goulden et al., 2014; Sridharan et al., 2008; van den Heuvel et al., 2009).

Previous RSFC studies showed that the AI might modulate the activity of the CEN and DMN and facilitate network switching between the DMN and CEN (Moran et al., 2013; Sridharan et al., 2008; Uddin et al., 2011). According to the triple-network model proposed by Menon and Uddin (2010), the AI mediates dynamic interactions between networks, detecting salient stimuli and initiating control signals to the CEN and DMN for externally-oriented attention and internal-related states. The CEN, mainly comprising the dorsolateral prefrontal cortex and posterior parietal cortex, is thought to associate with active maintenance, information manipulation, and decision-making of goal-driven behaviors (Moran et al., 2013; Sridharan et al., 2008; Uddin et al., 2011). In the current study, we detected lower RSFC between the AI and superior and inferior parietal cortices adjacent to the occipital cortex (Fig. 3), components of the CEN, in BD-II patients. Menon (Menon, 2011) suggested that abnormal RSFC between the AI and CEN may be associated with aberrant salience detection and engagement of executive functions, including inappropriate cognition and maladaptive goal-driven behaviors in psychiatric illnesses.

We also found lower RSFC between the left AI and occipital cortices, which include LOC, LG, and FG, in the BD-II patients than the controls (Fig. 3). The LOC, LG, and FG belong to the occipitoparietal visual region (Thomas Yeo et al., 2011) and are highly connected with the insula (Ghaziri et al., 2015). In a multisensory perceptual model (Sterzer and Kleinschmidt, 2010), the AI is suggested to be capable of detecting multiple sensory signals from the visual, auditory, and somatosensory cortices and mediates states of alertness through its connections to sensory cortices. The AI may serve as an integrative node in sensory perception and action readiness (Sterzer and Kleinschmidt, 2010), and the abnormal connections between the AI and sensory cortices may reflect the disrupted sensory perception in BD-II patients (O'Bryan et al., 2014). For example, Pang et al. (2018) suggested that abnormal RSFC between the AI and sensory areas may result in depressive states in BD-II patients due to disruption in the external-orientated system (Goya-

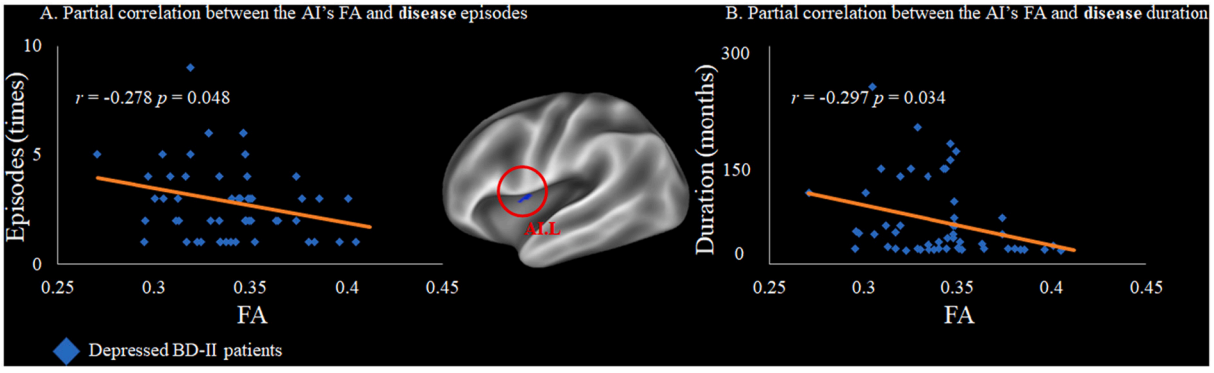

Fig. 4. Partial correlations between fractional anisotropy (FA) in the left anterior insula (AL.L) and clinical variables (disease episodes and duration time) for the patients with bipolar II disorder (BD-II).

Maldonado et al., 2016). Taking these findings together, we might suggest that the lower RSFC between the left AI and the left superior and inferior parietal cortices and occipital visual cortices may reflect a disrupted regulation in attentional orientation to salient external stimuli in BD-II patients.

4.2. Left-lateralized AI abnormality

The current study also showed the abnormal structure in the left AI for patients with BD-II depression. About the left-lateralized AI abnormality, several studies (Craig, 2005; Duerden et al., 2013) suggested that it may be associated with valance-specific stimuli (positive or negative) and behaviors (approach or withdrawal). For example, stimulation in the left AI may be associated with positive affect and approach behaviors involving the parasympathetic system(Craig, 2005). The decreased RSFC between the left AI and CEN has been reported in both BD patients with depression and MDD patients with depression compared with healthy controls, suggesting a disrupted functional pattern in response to salient stimuli (Ellard et al., 2018).

4.3. Abnormal cortical area in the left PCC in depressed BD-II patients

Our study also showed that patients with BD-II depression showed lower RSFC between the left PCC and right mPFC than the controls (Fig. 3). Both PCC and mPFC are identified as midline nodes of the DMN, which shows a dynamic pattern of activity during cognition in which it becomes relatively less active during the performance of active cognitive tasks (Gusnard et al., 2001). The DMN is involved in internally-directed thoughts (Buckner et al., 2008), such as daydreaming, autobiographical memory retrieval, and future planning (Addis et al., 2007; Gusnard et al., 2001; Mason et al., 2007). Aberrant DMN activities may underlie several dysfunctional psychological processes in self-referential processing, working memory, and attentional control, which have been commonly related to mental disorders such as schizophrenia, bipolar, and depression (Broyd et al., 2009). For example, aberrant DMN activation and connectivity, especially the PCC-mPFC RSFC aberration, have been related to trait rumination in depressed patients (Berman et al., 2010; Cooney et al., 2010). Rumination, a characteristic of depression, is a tendency to repetitively and passively focus on negative moods and their causes and adverse consequences (Nolen-Hoeksema et al., 2008). High levels of rumination are related to more prolonged and severe depressive symptoms, an increased risk for depression relapse, and are a key factor in the development of depression (Michalak et al., 2011).

In the current study, the depressed BD-II patients showed lower RSFC between the PCC and mPFC (posterior and anterior DMN) relative to the healthy controls, which was largely consistent with previous studies (Connolly et al., 2013; Lois and Wessa, 2016). For example, Lois and Wessa (2016) found depressed patients relative to controls showed lower posterior-anterior DMN RSFC, which in turn negatively correlated with rumination scores. Although there exists a discrepancy in the direction of RSFC change in DMN in depression (Berman et al., 2010; Connolly et al., 2013; Ho et al., 2015; Lois and Wessa, 2016), the result of the aberrant DMN RSFC, especially the PCC-mPFC RSFC, may relate to deficits in self-referential processing and associated with depressive symptoms like excessive self-focused and maladaptive rumination in BD-II depressive patients (Broyd et al., 2009; Ho et al., 2015).

4.4. Left-lateralized PCC abnormality

The current study revealed abnormal thickness and spontaneous brain activity in the left PCC (Fig. 3.). Similar results have also been reported in previous studies (Atmaca et al., 2007; Lu et al., 2014; Nugent et al., 2006; Zhong et al., 2019). However, the lateralized effect of PCC on BD is still not well-evidenced yet. Some studies (Kaur et al., 2005; Zhong et al., 2019) reported abnormal cortical thickness and spontaneous brain activity in the bilateral PCC, while other studies (Atmaca et al., 2007; Lu et al., 2014; Nugent et al., 2006) reported left-lateralized PCC's abnormality on BD pathophysiology. For instance, Atmaca et al. (2007) and Nugent et al. (2006) showed that un-medicated (drug-free) BD patients had smaller volumes in the left PCC compared with the medicated BD patients and controls. Lu et al. (2014) found decreased ALFF in the left precuneus in children with BD. Taken together, either left or bilateral cortical abnormalities of the PCC have been found in BD patients (Fountoulakis et al., 2008).

4.5. Comparisons to major depression disorder from previous literature

Some studies (Kupfer et al., 2012; Phillips and Kupfer, 2013) reported the altered structural and functional patterns for emotion regulation or reward processing in different types of mood disorders, which may be used to differentiate BD from MDD (Han et al., 2019). By taking the measures of brain gray matter volume and spontaneous neural activity ALFF, two meta-analyses studies reported that both disorders shared a common altered structural (Wise et al., 2017) and functional (Gong et al., 2020) pattern relative to controls involving the mPFC and bilateral insula. However, another meta-analysis (Pastrnak et al., 2021) collected studies involving comparisons of regional functional measures (degree centrality, regional homogeneity, and ALFF) between depressed BD and MDD and suggested that the increased neural activity in the left insula could be a biomarker for differentiating both disorders. These discrepancies may be due to variability of mood states and diversity of samples in BD patients (Han et al., 2019; Rive et al., 2015; Rive et al., 2016). Even though we did not perform a multimodal neuroimaging analysis between BD and MDD directly, our result of the abnormal patterns in the left AI and FC may provide new evidence for differentiating BD-II depression from MDD. In addition to the increased activity in the insula (Ambrosi et al., 2017; Li et al., 2017), evidence also revealed distinct insular connectivity patterns (Ellard et al., 2018; Pang et al., 2018) between BD and MDD patients. For example, Ellard et al. (2018) found that the significantly changed FC between the AI and inferior parietal cortex (IPC) may discriminate BD with MDD, and Pang et al. (2018) found that abnormal dynamic FC between the AI and sensory cortex may also be used to differentiate BD from MDD. Consistent with these findings, our results also revealed the abnormal connectivity between the AI and occipital and parietal cortices in the BD-II patients with depression. As for the discrepancies of the lateralized effects among these studies, the possible reason may be related to different analytical methods and sample variability. First, both Ellard et al. (2018) and Pang et al. (2018) performed FC analyses by using the pre-defined ROIs from previous studies rather than from the results based on their neuroimaging data. Second, the subtypes of BD were not consistent among these studies. Collectively, our finding showing multimodal brain differences in the left AI may suggest that the abnormal activity in the left AI could be a biomarker for characterizing depressed BD-II patients.

5. Limitations

This study has several limitations. Although our findings may relate to abnormal attentional orientation and self-referential thoughts in depressed BD-II patients, these abilities were not measured in our study and no direct analyses between imaging findings and behavioral performances were conducted. Future studies may consider including them in the research on BD-II and using common abnormal areas to classify or predict performances of these abilities on BD-II. Second, the sub-cortical structure was not included since the present study integrated and analyzed multimodal measures at the cortical surface. Previous studies (Phillips et al., 2008; Phillips and Swartz, 2014) also demonstrated neural circuits consisting of subcortical and cortical areas support emotional processing, emotional regulation, and reward processing. Future studies may consider involving cortico-subcortical circuits underlying BD-II. Third, although BD-II patients included in this study

were un-medicated for more than 6 months before the MRI scanning, the past medication levels could also influence the measured neuroimaging parameters. Unfortunately, we did not include this variable into consideration.

6. Conclusion

In conclusion, using cortical surface-based analysis, we identified the common abnormal areas in the left anterior insula and left posterior cingulate cortex by integrating multimodal MRI measures in depressed BD-II. We also found abnormal RSFC between the left AI and parietal as well as occipital cortices and between the left PCC and right mPFC in depressed BD-II. These results may indicate abnormal sensory perception and dysfunction of the attentional orientation to external stimuli and self-referential thoughts in depressed BD-II patients. The abnormalities of the left PCC and its connectivity with mPFC may associate with depressive symptoms in depressed BD-II patients. The abnormalities of the left AI and its connectivity with occipital and parietal cortices may serve as a neurobiomarker for distinguishing depressed BD-II from MDD.

Data availability statement

Data and code are available from the corresponding author upon reasonable request.

Author contributions

SZ, YW, RH, and LH designed the study; YW, SZ, GC, YJ, and LH assessed clinical diagnosis and collected MRI data; SZ, HH, and LC analyzed the data; SZ drafted the manuscript; RH, CS, Huiyuan, Huiqing, CL, YW, and Senning provided critical comments and revisions. All authors read and approved the final version of the manuscript for submission.

Ethical statements

This study was approved by the Institute Research Board of First Affiliated Hospital of Jinan University (FAHJU), Guangzhou. The written informed consent of each subject was acquired prior to the study.

Competing interests statement

The authors declare that they have no competing financial interests.

Acknowledgments

The study was supported by grants from the National Natural Science Foundation of China (82171914, 81871338, 81971597, 81471650, 81428013, and 81471654). The funding organizations played no further role in study design, data collection, analysis and interpretation, and paper writing.

References

Abé, C., Ekman, C.-J., Sellgren, C., Petrovic, P., Ingvar, M., Landén, M., 2016. Cortical thickness, volume and surface area in patients with bipolar disorder types I and II. J. Psychiatry Neurosci. 41 (4), 240–250. https://doi.org/10.1503/jpn.150093.

Abé, C., Rolstad, S., Petrovic, P., Ekman, C.J., Sparding, T., Ingvar, M., Landén, M., 2018. Bipolar disorder type I and II show distinct relationships between cortical thickness and executive function. Acta Psychiatr. Scand. 138 (4), 325–335. https://doi.org/10.1111/acps.12922.

Addis, D.R., Wong, A.T., Schacter, D.L., 2007. Remembering the past and imagining the future: common and distinct neural substrates during event construction and elaboration. Neuropsychologia 45 (7), 1363–1377. https://doi.org/10.1016/j.neuropsychologia.2006.10.016.

Adolfi, F., Couto, B., Richter, F., Decety, J., Lopez, J., Sigman, M., Ibáñez, A., 2017. Convergence of interoception, emotion, and social cognition: a twofold fMRI meta-analysis and lesion approach. Cortex 88, 124–142. https://doi.org/10.1016/j.cortex.2016.12.019.

Ambrosi, E., Rossi-Espagnet, M.C., Kotzalidis, G.D., Comparelli, A., Del Casale, A., Carducci, F., Girardi, P., 2013. Structural brain alterations in bipolar disorder II: a combined voxel-based morphometry (VBM) and diffusion tensor imaging (DTI) study. J. Affect. Disord. 150 (2), 610–615. https://doi.org/10.1016/j.jad.2013.02.023.

Ambrosi, E., Chiapponi, C., Sani, G., Manfredi, G., Piras, F., Caltagirone, C., Spalletta, G., 2016. White matter microstructural characteristics in bipolar I and bipolar II disorder: a diffusion tensor imaging study. J. Affect. Disord. 189, 176–183. https://doi.org/10.1016/j.jad.2015.09.035.

Ambrosi, E., Arciniegas, D.B., Madan, A., Curtis, K.N., Patriquin, M.A., Jorge, R.E., Salas, R., 2017. Insula and amygdala resting-state functional connectivity differentiate bipolar from unipolar depression. Acta Psychiatr. Scand. 136 (1), 129-139. https://doi.org/10.1111/acps.12724.

Association, A.P., 2000. Diagnostic criteria from dsM-iV-tr. American Psychiatric Pub.

Atmaca, M., Ozdemir, H., Cetinkaya, S., Parmaksiz, S., Belli, H., Kursad Poyraz, A., Ogur, E., 2007. Cingulate gyrus volumetry in drug free bipolar patients and patients treated with valproate or valproate and quetiapine. J. Psychiatr. Res. 41 (10), 821–827. https://doi.org/10.1016/j.jpsychires.2006.07.006.

Berman, M.G., Peltier, S., Nee, D.E., Kross, E., Deldin, P.J., Jonides, J., 2010. Depression, rumination and the default network. Soc. Cogn. Affect. Neurosci. 6 (5), 548–555. https://doi.org/10.1093/scan/nsq080.

Bora, E., Fornito, A., Yücel, M., Pantelis, C., 2010. Voxelwise meta-analysis of gray matter abnormalities in bipolar disorder. Biol. Psychiatry 67 (11), 1097–1105. https://doi.org/10.1016/j.biopsych.2010.01.020.

Brodoehl, S., Gaser, C., Dahnke, R., Witte, O.W., Klingner, C.M., 2020. Surface-based analysis increases the specificity of cortical activation patterns and connectivity results. Sci. Rep. 10 (1), 5737. https://doi.org/10.1038/s41598-020-62832-z.

Broyd, S.J., Demanuele, C., Debener, S., Helps, S.K., James, C.J., Sonuga-Barke, E.J.S., 2009. Default-mode brain dysfunction in mental disorders: a systematic review. Neurosci. Biobehav. Rev. 33 (3), 279–296. https://doi.org/10.1016/j.neubiorev.2008.09.002.

Buckner, R.L., Andrews-Hanna, J.R., Schacter, D.L., 2008. The brain's default network. Ann. N. Y. Acad. Sci. 1124 (1), 1–38. https://doi.org/10.1196/annals.1440.011.

Calhoun, V.D., Sui, J., 2016. Multimodal fusion of brain imaging data: a key to finding the missing link(s) in complex mental illness. Biol. Psychiatry: Cogn. Neurosci. Neuroimaging 1 (3), 230–244. https://doi.org/10.1016/j.bpsc.2015.12.005.

Caseras, X., Lawrence, N.S., Murphy, K., Wise, R.G., Phillips, M.L., 2013. Ventral striatum activity in response to reward: differences between bipolar I and II disorders. Am. J. Psychiatr. 170 (5), 533–541. https://doi.org/10.1176/appi.ajp.2012.12020169.

Chica, A.B., Bartolomeo, P., Lupiáñez, J., 2013. Two cognitive and neural systems for endogenous and exogenous spatial attention. Behav. Brain Res. 237, 107–123. https://doi.org/10.1016/j.bbr.2012.09.027.

Coalson, T.S., Van Essen, D.C., Glasser, M.F., 2018. The impact of traditional neuroimaging methods on the spatial localization of cortical areas. Proc. Natl. Acad. Sci. 115 (27), E6356. https://doi.org/10.1073/pnas.1801582115.

Connolly, C.G., Wu, J., Ho, T.C., Hoeft, F., Wolkowitz, O., Eisendrath, S., Yang, T.T., 2013. Resting-state functional connectivity of subgenual anterior cingulate cortex in depressed adolescents. Biol. Psychiatry 74 (12), 898–907. https://doi.org/10.1016/j.biopsych.2013.05.036.

Cooney, R.E., Joormann, J., Eugène, F., Dennis, E.L., Gotlib, I.H., 2010. Neural correlates of rumination in depression. Cogn. Affect. Behav. Neurosci. 10 (4), 470–478. https://doi.org/10.3758/CABN.10.4.470.

Craig, A.D., 2003. Interoception: the sense of the physiological condition of the body. Curr. Opin. Neurobiol. 13 (4), 500–505. https://doi.org/10.1016/S0959-4388(03)00090-4.

Craig, A.D., 2005. Forebrain emotional asymmetry: a neuroanatomical basis? Trends Cogn. Sci. 9 (12), 566–571. https://doi.org/10.1016/j.tics.2005.10.005.

Craig, A.D., 2009. How do you feel — now? The anterior insula and human awareness. Nat. Rev. Neurosci. 10 (1), 59–70. https://doi.org/10.1038/nrn2555.

Dale, A.M., Fischl, B., Sereno, M.I., 1999. Cortical surface-based analysis: I. Segmentation and surface reconstruction. Neuroimage 9 (2), 179–194. https://doi.org/10.1006/nimg.1998.0395.

Desikan, R.S., Ségonne, F., Fischl, B., Quinn, B.T., Dickerson, B.C., Blacker, D., Killiany, R.J., 2006. An automated labeling system for subdividing the human cerebral cortex on MRI scans into gyral based regions of interest. Neuroimage 31 (3), 968–980. https://doi.org/10.1016/j.neuroimage.2006.01.021.

Duerden, E.G., Arsalidou, M., Lee, M., Taylor, M.J., 2013. Lateralization of affective processing in the insula. Neuroimage 78, 159–175. https://doi.org/10.1016/j.neuroimage.2013.04.014.

Ellard, K.K., Zimmerman, J.P., Kaur, N., Van Dijk, K.R.A., Roffman, J.L., Nierenberg, A. A., Camprodon, J.A., 2018. Functional connectivity between anterior insula and key nodes of Frontoparietal executive control and salience networks distinguish bipolar depression from unipolar depression and healthy control subjects. Biol. Psychiatry Cogn. Neurosci. Neuroimaging 3 (5), 473–484. https://doi.org/10.1016/j.bpsc.2018.01.013.

Fountoulakis, K.N., Giannakopoulos, P., Kövari, E., Bouras, C., 2008. Assessing the role of cingulate cortex in bipolar disorder: neuropathological, structural and functional imaging data. Brain Res. Rev. 59 (1), 9–21. https://doi.org/10.1016/j.brainresrev.2008.04.005.

Ganzola, R., Duchesne, S., 2017. Voxel-based morphometry meta-analysis of gray and white matter finds significant areas of differences in bipolar patients from healthy controls. Bipolar Disord. 19 (2), 74–83. https://doi.org/10.1111/bdi.12488.

Ghaziri, J., Tucholka, A., Girard, G., Houde, J.-C., Boucher, O., Gilbert, G., Nguyen, D.K., 2015. The corticocortical structural connectivity of the human insula. Cereb. Cortex 27 (2), 1216–1228. https://doi.org/10.1093/cercor/bhv308.

Glasser, M.F., Sotiropoulos, S.N., Wilson, J.A., Coalson, T.S., Fischl, B., Andersson, J.L., Jenkinson, M., 2013. The minimal preprocessing pipelines for the human connectome project. Neuroimage 80, 105–124. https://doi.org/10.1016/j.neuroimage.2013.04.127.

Glasser, M.F., Coalson, T.S., Robinson, E.C., Hacker, C.D., Harwell, J., Yacoub, E., Van Essen, D.C., 2016a. A multi-modal parcellation of human cerebral cortex. Nature 536 (7615), 171–178. https://doi.org/10.1038/nature18933.

Glasser, M.F., Smith, S.M., Marcus, D.S., Andersson, J.L.R., Auerbach, E.J., Behrens, T.E. J., Van Essen, D.C., 2016b. The human connectome project's neuroimaging approach. Nat. Neurosci. 19 (9), 1175–1187. https://doi.org/10.1038/nn.4361.

Gong, J., Chen, G., Jia, Y., Zhong, S., Zhao, L., Luo, X., Wang, Y., 2019. Disrupted functional connectivity within the default mode network and salience network in unmedicated bipolar II disorder. Prog. Neuro-Psychopharmacol. Biol. Psychiatry 88, 11–18. https://doi.org/10.1016/j.pnpbp.2018.06.012.

Gong, J., Wang, J., Qiu, S., Chen, P., Luo, Z., Wang, J., Wang, Y., 2020. Common and distinct patterns of intrinsic brain activity alterations in major depression and bipolar disorder: voxel-based meta-analysis. Transl. Psychiatry 10 (1), 353. https://doi.org/10.1038/s41398-020-01036-5.

Goodkind, M., Eickhoff, S.B., Oathes, D.J., Jiang, Y., Chang, A., Jones-Hagata, L.B., Etkin, A., 2015. Identification of a common neurobiological substrate for mental illness. JAMA Psychiatry 72 (4), 305–315. https://doi.org/10.1001/jamapsychiatry.2014.2206.

Goulden, N., Khusnulina, A., Davis, N.J., Bracewell, R.M., Bokde, A.L., McNulty, J.P., Mullins, P.G., 2014. The salience network is responsible for switching between the default mode network and the central executive network: replication from DCM. Neuroimage 99, 180–190. https://doi.org/10.1016/j.neuroimage.2014.05.052.

Goya-Maldonado, R., Brodmann, K., Keil, M., Trost, S., Dechent, P., Gruber, O., 2016. Differentiating unipolar and bipolar depression by alterations in large-scale brain networks. Hum. Brain Mapp. 37 (2), 808–818. https://doi.org/10.1002/hbm.23070.

Guevara, M., Román, C., Houenou, J., Duclap, D., Poupon, C., Mangin, J.F., Guevara, P., 2017. Reproducibility of superficial white matter tracts using diffusion-weighted imaging tractography. Neuroimage 147, 703–725. https://doi.org/10.1016/j.neuroimage.2016.11.066.

Guevara, M., Guevara, P., Román, C., Mangin, J.-F., 2020. Superficial white matter: a review on the dMRI analysis methods and applications. Neuroimage 212, 116673. https://doi.org/10.1016/j.neuroimage.2020.116673.

Gusnard, D.A., Akbudak, E., Shulman, G.L., Raichle, M.E., 2001. Medial prefrontal cortex and self-referential mental activity: relation to a default mode of brain function. Proc. Natl. Acad. Sci. 98 (7), 4259–4264. https://doi.org/10.1073/pnas.071043098.

Ha, T.H., Ha, K., Kim, J.H., Choi, J.E., 2009. Regional brain gray matter abnormalities in patients with bipolar II disorder: a comparison study with bipolar I patients and healthy controls. Neurosci. Lett. 456 (1), 44–48. https://doi.org/10.1016/j.neulet.2009.03.077.

Han, K.-M., De Berardis, D., Fornaro, M., Kim, Y.-K., 2019. Differentiating between bipolar and unipolar depression in functional and structural MRI studies. Prog. Neuro-Psychopharmacol. Biol. Psychiatry 91, 20–27. https://doi.org/10.1016/j.pnpbp.2018.03.022.

Hanford, L.C., Nazarov, A., Hall, G.B., Sassi, R.B., 2016. Cortical thickness in bipolar disorder: a systematic review. Bipolar Disord. 18 (1), 4–18. https://doi.org/10.1111/bdi.12362.

Harrison, N.A., Gray, M.A., Gianaros, P.J., Critchley, H.D., 2010. The embodiment of emotional feelings in the brain. J. Neurosci. 30 (38), 12878–12884. https://doi.org/10.1523/JNEUROSCI.1725-10.2010.

Hibar, D.P., Westlye, L.T., Doan, N.T., Jahanshad, N., Cheung, J.W., Ching, C.R.K., for the, E. B. D. W. G, 2018. Cortical abnormalities in bipolar disorder: an MRI analysis of 6503 individuals from the ENIGMA Bipolar Disorder Working Group. Mol. Psychiatry 23 (4), 932–942. https://doi.org/10.1038/mp.2017.73.

Hirschfeld, R.M.A., Lewis, L., Vornik, L.A., 2003. Perceptions and impact of bipolar disorder: how far have we really come? Results of the National Depressive and Manic-Depressive Association 2000 survey of individuals with bipolar disorder. J. Clin. Psychiatry 64 (2), 161–174. https://doi.org/10.4088/JCP.v64n0209.

Ho, T.C., Connolly, C.G., Henje Blom, E., LeWinn, K.Z., Strigo, I.A., Paulus, M.P., Yang, T. T., 2015. Emotion-dependent functional connectivity of the default mode network in adolescent depression. Biol. Psychiatry 78 (9), 635–646. https://doi.org/10.1016/j.biopsych.2014.09.002.

Hong, S.-J., Hyung, B., Paquola, C., Bernhardt, B.C., 2018. The superficial white matter in autism and its role in connectivity anomalies and symptom severity. Cereb. Cortex 29 (10), 4415–4425. https://doi.org/10.1093/cercor/bhy321.

Iaria, G., Committeri, G., Pastorelli, C., Pizzamiglio, L., Watkins, K.E., Carota, A., 2008. Neural activity of the anterior insula in emotional processing depends on the individuals' emotional susceptibility. Hum. Brain Mapp. 29 (3), 363–373. https://doi.org/10.1002/hbm.20393.

Ji, E., Guevara, P., Guevara, M., Grigis, A., Labra, N., Sarrazin, S., Houenou, J., 2019. Increased and decreased superficial white matter structural connectivity in schizophrenia and bipolar disorder. Schizophr. Bull. 45 (6), 1367–1378. https://doi.org/10.1093/schbul/sbz015.

Judd, L.L., Schettler, P.J., Akiskal, H.S., Maser, J., Coryell, W., Solomon, D., Keller, M., 2003. Long-term symptomatic status of bipolar I vs. bipolar II disorders. Int. J. Neuropsychopharmacol. 6 (2), 127–137. https://doi.org/10.1017/S1461145703003341.

Kaur, S., Sassi, R.B., Axelson, D., Nicoletti, M., Brambilla, P., Monkul, E.S., Soares, J.C., 2005. Cingulate cortex anatomical abnormalities in children and adolescents with bipolar disorder. Am. J. Psychiatr. 162 (9), 1637–1643. https://doi.org/10.1176/appi.ajp.162.9.1637.

Kupfer, D.J., Frank, E., Phillips, M.L., 2012. Major depressive disorder: new clinical, neurobiological, and treatment perspectives. Lancet 379 (9820), 1045–1055. https://doi.org/10.1016/S0140-6736(11)60602-8.

Kurumaji, A., Itasaka, M., Uezato, A., Takiguchi, K., Jitoku, D., Hobo, M., Nishikawa, T., 2017. A distinctive abnormality of diffusion tensor imaging parameters in the fornix of patients with bipolar II disorder. Psychiatry Res. Neuroimaging 266, 66–72. https://doi.org/10.1016/j.pscychresns.2017.06.005.

Li, M., Das, T., Deng, W., Wang, Q., Li, Y., Zhao, L., Li, T., 2017. Clinical utility of a short resting-state MRI scan in differentiating bipolar from unipolar depression. Acta Psychiatr. Scand. 136 (3), 288–299. https://doi.org/10.1111/acps.12752.

Liu, M., Bernhardt, B.C., Hong, S.-J., Caldairou, B., Bernasconi, A., Bernasconi, N., 2016. The superficial white matter in temporal lobe epilepsy: a key link between structural and functional network disruptions. Brain 139 (9), 2431–2440. https://doi.org/10.1093/brain/aww167.

Liu, S., Wang, H., Song, M., Lv, L., Cui, Y., Liu, Y., Sui, J., 2018. Linked 4-way multimodal brain differences in schizophrenia in a large Chinese Han population. Schizophr. Bull. 45 (2), 436–449. https://doi.org/10.1093/schbul/sby045.

Lois, G., Wessa, M., 2016. Differential association of default mode network connectivity and rumination in healthy individuals and remitted MDD patients. Soc. Cogn. Affect. Neurosci. 11 (11), 1792–1801. https://doi.org/10.1093/scan/nsw085.

Lu, D., Jiao, Q., Zhong, Y., Gao, W., Xiao, Q., Liu, X., Su, L., 2014. Altered baseline brain activity in children with bipolar disorder during mania state: a resting-state study. Neuropsychiatr. Dis. Treat. 10, 317–323. https://doi.org/10.2147/NDT.S54663.

Maller, J.J., Thaveenthiran, P., Thomson, R.H., McQueen, S., Fitzgerald, P.B., 2014. Volumetric, cortical thickness and white matter integrity alterations in bipolar disorder type I and II. J. Affect. Disord. 169, 118–127. https://doi.org/10.1016/j.jad.2014.08.016.

Marcus, D.S., Harms, M.P., Snyder, A.Z., Jenkinson, M., Wilson, J.A., Glasser, M.F., Van Essen, D.C., 2013. Human connectome project informatics: quality control, database services, and data visualization. Neuroimage 80, 202–219. https://doi.org/10.1016/j.neuroimage.2013.05.077.

Mason, M.F., Norton, M.I., Van Horn, J.D., Wegner, D.M., Grafton, S.T., Macrae, C.N., 2007. Wandering minds: the default network and stimulus-independent thought. Science 315 (5810), 393–395. https://doi.org/10.1126/science.1131295.

Meng, X., Jiang, R., Lin, D., Bustillo, J., Jones, T., Chen, J., Calhoun, V.D., 2017. Predicting individualized clinical measures by a generalized prediction framework and multimodal fusion of MRI data. Neuroimage 145, 218–229. https://doi.org/10.1016/j.neuroimage.2016.05.026.

Menon, V., 2011. Large-scale brain networks and psychopathology: a unifying triple network model. Trends Cogn. Sci. 15 (10), 483–506. https://doi.org/10.1016/j.tics.2011.08.003.

Menon, V., Uddin, L.Q., 2010. Saliency, switching, attention and control: a network model of insula function. Brain Struct. Funct. 214 (5), 655–667. https://doi.org/10.1007/s00429-010-0262-0.

Merikangas, K.R., Jin, R., He, J.-P., Kessler, R.C., Lee, S., Sampson, N.A., Zarkov, Z., 2011. Prevalence and correlates of bipolar spectrum disorder in the world mental health survey initiative. Arch. Gen. Psychiatry 68 (3), 241–251. https://doi.org/10.1001/archgenpsychiatry.2011.12.

Michalak, J., Hölz, A., Teismann, T., 2011. Rumination as a predictor of relapse in mindfulness-based cognitive therapy for depression. Psychol. Psychother. Theory Res. Pract. 84 (2), 230–236. https://doi.org/10.1348/147608310X520166.

Moran, L.V., Tagamets, M.A., Sampath, H., O'Donnell, A., Stein, E.A., Kochunov, P., Hong, L.E., 2013. Disruption of anterior insula modulation of large-scale brain networks in schizophrenia. Biol. Psychiatry 74 (6), 467–474. https://doi.org/10.1016/j.biopsych.2013.02.029.

Nazeri, A., Chakravarty, M.M., Felsky, D., Lobaugh, N.J., Rajji, T.K., Mulsant, B.H., Voineskos, A.N., 2013. Alterations of superficial white matter in schizophrenia and relationship to cognitive performance. Neuropsychopharmacology 38 (10), 1954–1962. https://doi.org/10.1038/npp.2013.93.

Nazeri, A., Chakravarty, M.M., Rajji, T.K., Felsky, D., Rotenberg, D.J., Mason, M., Voineskos, A.N., 2015. Superficial white matter as a novel substrate of age-related cognitive decline. Neurobiol. Aging 36 (6), 2094–2106. https://doi.org/10.1016/j.neurobiolaging.2015.02.022.

Nolen-Hoeksema, S., Wisco, B.E., Lyubomirsky, S., 2008. Rethinking rumination. Perspect. Psychol. Sci. 3 (5), 400–424. https://doi.org/10.1111/j.1745-6924.2008.00088.x.

Nugent, A.C., Milham, M.P., Bain, E.E., Mah, L., Cannon, D.M., Marrett, S., Drevets, W.C., 2006. Cortical abnormalities in bipolar disorder investigated with MRI and voxel-based morphometry. Neuroimage 30 (2), 485–497. https://doi.org/10.1016/j.neuroimage.2005.09.029.

O'Bryan, R.A., Brenner, C.A., Hetrick, W.P., O'Donnell, B.F., 2014. Disturbances of visual motion perception in bipolar disorder. Bipolar Disord. 16 (4), 354–365. https://doi.org/10.1111/bdi.12173.

Oishi, K., Zilles, K., Amunts, K., Faria, A., Jiang, H., Li, X., Mori, S., 2008. Human brain white matter atlas: identification and assignment of common anatomical structures in superficial white matter. Neuroimage 43 (3), 447–457. https://doi.org/10.1016/j.neuroimage.2008.07.009.

Oosterhof, N.N., Wiestler, T., Downing, P.E., Diedrichsen, J., 2011. A comparison of volume-based and surface-based multi-voxel pattern analysis. Neuroimage 56 (2), 593–600. https://doi.org/10.1016/j.neuroimage.2010.04.270.

Pang, Y., Chen, H., Wang, Y., Long, Z., He, Z., Zhang, H., Chen, H., 2018. Transdiagnostic and diagnosis-specific dynamic functional connectivity anchored in the right anterior insula in major depressive disorder and bipolar depression. Prog. Neuro-

Psychopharmacol. Biol. Psychiatry 85, 7–15. https://doi.org/10.1016/j.pnpbp.2018.03.020.
Pastrnak, M., Simkova, E., Novak, T., 2021. Insula activity in resting-state differentiates bipolar from unipolar depression: a systematic review and meta-analysis. Sci. Rep. 11 (1), 16930. https://doi.org/10.1038/s41598-021-96319-2.
Phillips, M.L., Kupfer, D.J., 2013. Bipolar disorder diagnosis: challenges and future directions. Lancet 381 (9878), 1663–1671. https://doi.org/10.1016/S0140-6736(13)60989-7.
Phillips, M.L., Swartz, H.A., 2014. A critical appraisal of neuroimaging studies of bipolar disorder: toward a new conceptualization of underlying neural circuitry and a road map for future research. Am. J. Psychiatr. 171 (8), 829–843. https://doi.org/10.1176/appi.ajp.2014.13081008.
Phillips, M.L., Ladouceur, C.D., Drevets, W.C., 2008. A neural model of voluntary and automatic emotion regulation: implications for understanding the pathophysiology and neurodevelopment of bipolar disorder. Mol. Psychiatry 13 (9), 833–857. https://doi.org/10.1038/mp.2008.65.
Phillips, O.R., Joshi, S.H., Piras, F., Orfei, M.D., Iorio, M., Narr, K.L., Di Paola, M., 2016a. The superficial white matter in Alzheimer's disease. Hum. Brain Mapp. 37 (4), 1321–1334. https://doi.org/10.1002/hbm.23105.
Phillips, O.R., Joshi, S.H., Squitieri, F., Sanchez-Castaneda, C., Narr, K., Shattuck, D.W., Di Paola, M., 2016b. Major Superficial White Matter Abnormalities in Huntington's Disease [Original Research]. Front. Neurosci. 10 (197) https://doi.org/10.3389/fnins.2016.00197.
Rive, M.M., Mocking, R.J.T., Koeter, M.W.J., van Wingen, G., de Wit, S.J., van den Heuvel, O.A., Schene, A.H., 2015. State-dependent differences in emotion regulation between unmedicated bipolar disorder and major depressive disorder. JAMA Psychiatry 72 (7), 687–696. https://doi.org/10.1001/jamapsychiatry.2015.0161.
Rive, M.M., Redlich, R., Schmaal, L., Marquand, A.F., Dannlowski, U., Grotegerd, D., Ruhé, H.G., 2016. Distinguishing medication-free subjects with unipolar disorder from subjects with bipolar disorder: state matters. Bipolar Disord. 18 (7), 612-623. https://doi.org/10.1111/bdi.12446.
Robinson, E.C., Garcia, K., Glasser, M.F., Chen, Z., Coalson, T.S., Makropoulos, A., Rueckert, D., 2018. Multimodal surface matching with higher-order smoothness constraints. Neuroimage 167, 453–465. https://doi.org/10.1016/j.neuroimage.2017.10.037.
Schüz, A., Braitenberg, V., 2002. The human cortical white matter: quantitative aspects of cortico-cortical long-range connectivity. Cortical Areas Unity Divers. 377-385 https://doi.org/10.1201/9780203299296.
Sridharan, D., Levitin, D.J., Menon, V., 2008. A critical role for the right fronto-insular cortex in switching between central-executive and default-mode networks. Proc. Natl. Acad. Sci. 105 (34), 12569–12574. https://doi.org/10.1073/pnas.0800005105.
Sterzer, P., Kleinschmidt, A., 2010. Anterior insula activations in perceptual paradigms: often observed but barely understood. Brain Struct. Funct. 214 (5), 611–622. https://doi.org/10.1007/s00429-010-0252-2.
Sui, J., Huster, R., Yu, Q., Segall, J.M., Calhoun, V.D., 2014. Function–structure associations of the brain: evidence from multimodal connectivity and covariance studies. Neuroimage 102, 11–23. https://doi.org/10.1016/j.neuroimage.2013.09.044.
Sui, J., Pearlson, G.D., Du, Y., Yu, Q., Jones, T.R., Chen, J., Calhoun, V.D., 2015. In search of multimodal neuroimaging biomarkers of cognitive deficits in schizophrenia. Biol. Psychiatry 78 (11), 794–804. https://doi.org/10.1016/j.biopsych.2015.02.017.
Sui, J., Qi, S., van Erp, T.G.M., Bustillo, J., Jiang, R., Lin, D., Calhoun, V.D., 2018. Multimodal neuromarkers in schizophrenia via cognition-guided MRI fusion. Nat. Commun. 9 (1), 3028–3041. https://doi.org/10.1038/s41467-018-05432-w.
Thomas Yeo, B.T., Krienen, F.M., Sepulcre, J., Sabuncu, M.R., Lashkari, D., Hollinshead, M., Buckner, R.L., 2011. The organization of the human cerebral cortex estimated by intrinsic functional connectivity. J. Neurophysiol. 106 (3), 1125–1165. https://doi.org/10.1152/jn.00338.2011.
Uddin, L.Q., Supekar, K.S., Ryali, S., Menon, V., 2011. Dynamic reconfiguration of structural and functional connectivity across core neurocognitive brain networks with development. J. Neurosci. 31 (50), 18578–18589. https://doi.org/10.1523/JNEUROSCI.4465-11.2011.
van den Heuvel, M.P., Mandl, R.C.W., Kahn, R.S., Hulshoff Pol, H.E., 2009. Functionally linked resting-state networks reflect the underlying structural connectivity architecture of the human brain. Hum. Brain Mapp. 30 (10), 3127–3141. https://doi.org/10.1002/hbm.20737.
Van Essen, D.C., 2004. Surface-based approaches to spatial localization and registration in primate cerebral cortex. Neuroimage 23, S97–S107. https://doi.org/10.1016/j.neuroimage.2004.07.024.
Van Essen, D.C., 2012. Cortical cartography and Caret software. Neuroimage 62 (2), 757–764. https://doi.org/10.1016/j.neuroimage.2011.10.077.
Van Essen, D.C., Smith, S.M., Barch, D.M., Behrens, T.E.J., Yacoub, E., Ugurbil, K., 2013. The WU-Minn human connectome project: an overview. Neuroimage 80, 62–79. https://doi.org/10.1016/j.neuroimage.2013.05.041.
Vizueta, N., Rudie, J.D., Townsend, J.D., Torrisi, S., Moody, T.D., Bookheimer, S.Y., Altshuler, L.L., 2012. Regional fMRI hypoactivation and altered functional connectivity during emotion processing in nonmedicated depressed patients with bipolar II disorder. Am. J. Psychiatr. 169 (8), 831–840. https://doi.org/10.1176/appi.ajp.2012.11030349.
Wang, Y., Zhong, S., Jia, Y., Sun, Y., Wang, B., Liu, T., Huang, L., 2016. Disrupted resting-state functional connectivity in nonmedicated bipolar disorder. Radiology 280 (2), 529–536. https://doi.org/10.1148/radiol.2016151641.
Wang, Y., Sun, K., Liu, Z., Chen, G., Jia, Y., Zhong, S., Tian, J., 2019a. Classification of unmedicated bipolar disorder using whole-brain functional activity and connectivity: a radiomics analysis. Cereb. Cortex 30 (3), 1117–1128. https://doi.org/10.1093/cercor/bhz152.
Wang, J., Wang, Y., Huang, H., Jia, Y., Zheng, S., Zhong, S., Huang, R., 2019b. Abnormal dynamic functional network connectivity in unmedicated bipolar and major depressive disorders based on the triple-network model. Psychol. Med. 1-10 https://doi.org/10.1017/S003329171900028X.
Williams, J.B.W., 1988. A structured interview guide for the Hamilton depression rating scale. Arch. Gen. Psychiatry 45 (8), 742–747. https://doi.org/10.1001/archpsyc.1988.01800320058007.
Winkler, A.M., Ridgway, G.R., Webster, M.A., Smith, S.M., Nichols, T.E., 2014. Permutation inference for the general linear model. Neuroimage 92, 381–397. https://doi.org/10.1016/j.neuroimage.2014.01.060.
Winkler, A.M., Webster, M.A., Brooks, J.C., Tracey, I., Smith, S.M., Nichols, T.E., 2016. Non-parametric combination and related permutation tests for neuroimaging. Hum. Brain Mapp. 37 (4), 1486–1511. https://doi.org/10.1002/hbm.23115.
Wise, T., Radua, J., Via, E., Cardoner, N., Abe, O., Adams, T.M., Arnone, D., 2017. Common and distinct patterns of grey-matter volume alteration in major depression and bipolar disorder: evidence from voxel-based meta-analysis. Mol. Psychiatry 22 (10), 1455–1463. https://doi.org/10.1038/mp.2016.72.
Xu, T., Opitz, A., Craddock, R.C., Wright, M.J., Zuo, X.-N., Milham, M.P., 2016. Assessing variations in areal organization for the intrinsic brain: from fingerprints to reliability. Cereb. Cortex 26 (11), 4192–4211. https://doi.org/10.1093/cercor/bhw241.
Yang, H., Long, X.-Y., Yang, Y., Yan, H., Zhu, C.-Z., Zhou, X.-P., Gong, Q.-Y., 2007. Amplitude of low frequency fluctuation within visual areas revealed by resting-state functional MRI. Neuroimage 36 (1), 144–152. https://doi.org/10.1016/j.neuroimage.2007.01.054.
Young, R.C., Biggs, J.T., Ziegler, V.E., Meyer, D.A., 1978. A rating scale for mania: reliability, validity and sensitivity. Br. J. Psychiatry 133 (5), 429–435. https://doi.org/10.1192/bjp.133.5.429.
Zhang, S., Wang, Y., Deng, F., Zhong, S., Chen, L., Luo, X., Huang, R., 2018. Disruption of superficial white matter in the emotion regulation network in bipolar disorder. NeuroImage: Clin. 20, 875–882. https://doi.org/10.1016/j.nicl.2018.09.024.
Zhong, S., Chen, G., Zhao, L., Jia, Y., Chen, F., Qi, Z., Wang, Y., 2019. Correlation between intrinsic brain activity and thyroid-stimulating hormone level in unmedicated bipolar II depression. Neuroendocrinology 108 (3), 232–243. https://doi.org/10.1159/000497182.